



International Conference on Concentrating Solar Power and Chemical Energy Systems,
SolarPACES 2014

Investigation into the coupling of Micro Gas Turbines with CSP technology: OMSoP project

M. Lanchi^{a*}, M. Montecchi^a, T. Crescenzi^a, D. Mele^a, A. Miliozzi^a, V. Russo^a,
D. Mazzei^a, M. Misceo^a, M. Falchetta^a and R. Mancini^b

^aENEA – Italian National Agency for New Technology, Energy and Sustainable Economic Development, Casaccia Research Center, Via Anguillarese 301, 00123 S. Maria di Galeria, Rome (Italy), ^bTU/e Eindhoven University of Technology, Den Dolech 2, 5612 AZ Eindhoven, (Netherlands)

Abstract

Solar power generation has been gaining worldwide increasing interest by virtue of its ability to meet both the growing energy needs and the increasing concerns on the carbon dioxide emissions. One of the most promising Concentrated Solar Power (CSP) technologies under development uses a parabolic dish to concentrate solar power into a focal point, raising the temperature of a working fluid which is then used in a thermodynamic cycle to generate electricity. In the OMSoP project, funded by the European Commission, it is proposed to use a Brayton cycle in the form of a micro-gas turbine (MGT), which replaces the more conventional Stirling engine, with the aim of increasing the ratio of the electric power generated to the solar energy collected and improving the operability in relation to solar energy short time fluctuations. To achieve these objectives, research and development will be conducted in all aspects of the system leading to a full scale demonstrative plant to be located at the ENEA Casaccia Research Centre. The present work deals with the activities carried out so far by ENEA, which is principally involved in the development and experimental characterization of the dish component, and in the integration of the complete system, both in terms of modelling and realization.

© 2015 The Authors. Published by Elsevier Ltd. This is an open access article under the CC BY-NC-ND license (<http://creativecommons.org/licenses/by-nc-nd/4.0/>).

Peer review by the scientific conference committee of SolarPACES 2014 under responsibility of PSE AG

Keywords: CSP technology; Micro Gas Turbine; Dish-MGT coupling; Dish design; Ray-tracing method; System integration

* Corresponding author. Tel.: +39 (0)6 30483292; fax: +39 (0)6 30486779.
E-mail address: michela.lanchi@enea.it

1. Introduction

In the field of renewable energies the Concentrated Solar Power (CSP) technology can represent an important route to balance the increasing energy needs and the compelling problem of carbon dioxide emissions. This technology can be applied both for high capacity power plants, through the use of parabolic trough and solar tower systems in conjunction with steam turbines, and for small capacity applications through the adoption of dish systems, usually coupled with Stirling engines.

With regard to the dish-Stirling technology, the main research effort is presently focused on the improvement of the system operability which presents high complexity and poor reliability, as well as high cost. In the present work it is proposed to use a micro-gas turbine (MGT) in place of the more conventional Stirling engine, with the aim of increasing the ratio of the electric power generated to the solar energy collected and improving the operability in relation to solar energy short time fluctuations. The adoption of a MGT is a substantial innovation in the field of the dish technology but is in line with an increasing interest towards the solar gas turbine applications. In fact in the last years several projects focused on the integration of gas turbines with solar energy have been funded by the European Commission. In particular, within the SOLGATE [1] project, a solar-powered gas turbine has been developed. In 2010, the SOLHYCO [2] project carried out improvements on integrating a commercial co-generative micro-gas turbine with a new bio-fuel combustion system. These activities have led to a number of new projects that are currently under development, e.g. SHCC [3], SOLUGAS [4] and PEGASE [5]. However, even if the technical feasibility of MW scale power plants has been investigated so far, the use of micro-gas turbines with the solar source for distributed electricity production in remote areas is a new perspective.

Nomenclature

$A_{effective}$	Dish Effective Area	P_w	Power on the receiver window	U_{conv}	Heat transfer coefficient
A_w	Window aperture area	P_{coll}	Power collected on the mirror	α	Window absorbance
C	Concentration Factor	P_{abs}	Power transmitted to the cavity	ΔT_f	Temperature difference
CCD	Charge Coupling Device	PDC	Parabolic Dish Concentrator	$\varphi(\xi)$	Concentrated flux
CSP	Concentrated Solar Power	P_{conv}	Power lost by convection	Δs	Numerical resolution
D	Dish Diameter	P_{ele}	Electric power output	ε	Receiver emissivity
DNI	Direct Normal Irradiation	P_t	Total turbine power	η_r	Mirror reflectance
F	Focal distance	P_{cm}	Total compressor power	η_c	Compressor efficiency
h	Enthalpy	P_c	Compressor power	η_{ele}	Electrical efficiency
m_{air}	Air flowrate	RC	Ratio Captured	η_{mec}	Mechanical efficiency
MGT	Micro Gas Turbine	r_g	Radius of the focal spot	η_{rec}	Recuperator efficiency
S	Surface area	rpm	Speed rate	η_t	Turbine efficiency
P	Pressure	T	Temperature	η_{tot}	Total efficiency
P_r	Turbine expansion ratio	T_a	Ambient temperature	θ_s	Sun disk aperture angle
P_{ratio}	Compressor pressure ratio	TIT	Turbine Inlet Temperature	θ_{inc}	Angle of incidence
P_{in}	Total incident power	T_{sky}	Radiation reference	μ	Standard deviation
P_{reirr}	Power lost by radiation	Z	Receiver optimal position	σ	Stefan-Boltzman constant

2. OMSoP project description

The main objective of the OMSoP project, which has started in February 2013, is to develop and demonstrate advanced technical solutions for concentrated solar power systems coupled to MGT to produce electricity in the range of 3-10 kW. The system is destined to fulfil energy needs for domestic and small commercial applications while, for larger energy needs, the units can be stacked by virtue of their modular nature. Furthermore the proposed system can be integrated with medium and long term thermal storage or with a back-up system powered by conventional fuels or biofuels to assure electricity generation in the absence of solar insolation.

The principal technical challenge is to enable the production of small scale cost effective, efficient, reliable and easy to maintain units for either on or off-grid applications. The whole system will be built and tested at the ENEA Casaccia site (near Rome) to demonstrate its functionality. The consortium is composed of SMEs and Research institutions with a track record in all the aspects required to design, build and demonstrate the system (The City University, Università degli Studi Roma Tre, ENEA, Innova Solar Energy, Compower AB, Kungliga Tekniska Högskolan, Universidad de Sevilla, European Turbine Network). The main components of the system, whose conceptual layout is reported in Fig. 1, are the solar dish concentrator, the receiver and the MGT. The solar receiver, positioned in correspondence of the focal point of the dish, absorbs and converts the concentrated radiation into sensible heat of the working fluid, which is then processed by the MGT for producing electricity.

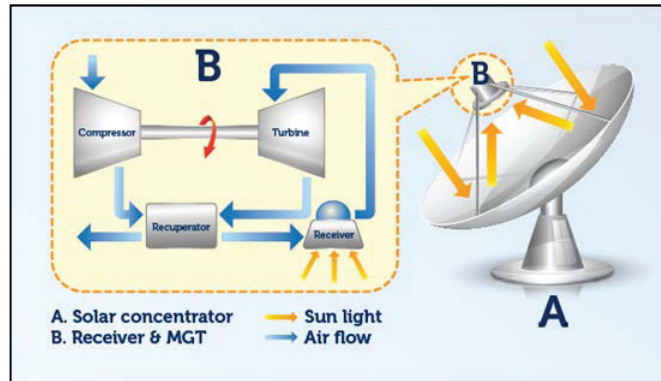


Fig. 1. Conceptual scheme of the OMSoP concentrating power system

The replacement of the Stirling engine, which is the most common technology, with a micro-gas turbine is a novel feature of the project: thanks to the MGT high power to weight ratio, simplicity of design and reliability, a relevant improvement in the technology is expected. Compower, which is the partner responsible for the heat engine realization, has recently developed a MGT in the power range below 10 kWe. Research, however, is required in order to select the optimum configuration of the MGT when coupled to a concentrating solar power (CSP) system. Issues to be investigated are the optimum Turbine Inlet Temperature (TIT), recuperation and the choice of closed or open cycle.

The integration between the solar receiver and the MGT represents the principal challenge of the project and a big chance at the same time: thanks to the compact design of the MGT it is possible to incorporate it into the receiver structure and to bring the turbine inlet temperature close to the receiver temperature, eliminating transmission losses. Another important objective is to improve the current receiver design to achieve receiver temperatures approaching 900°C in place of more common 800°C [2], in order to obtain higher cycle efficiency and to reduce the solar dish size. The receiver design and optimization activities are in charge of KTH and RO3.

The present work deals with the activities carried out so far by ENEA, which is principally involved in two tasks: 1) development and experimental characterization of the dish component, together with Innova, 2) system integration, realization and testing. Regarding the first point, as a first step a theoretical analysis of different dish configurations has been performed with the aim of increasing the dish efficiency maintaining a light and handy structure. The selected dish arrangement has been successively tailored to the MGT-receiver requirements. In particular the solar collector has been optimized in terms of shape and materials for achieving the target concentration factor and turbine inlet temperature (~900°C).

Regarding the system integration activity, ENEA has developed a complete system model both for predicting the behavior of the demo plant and for providing useful information for system components improvement. The commercial codes TRNSYS and EES have been selected for building the system model. In particular TRNSYS code, which is a dynamic simulation program primarily used in the field of renewable energy and solar applications, has been used for assembling a preliminary simplified tool, using the components available in the TRNSYS library. In a second step a more customized and detailed system has been built, integrating the component models developed mainly in EES as external subroutines.

3. Concentrator design

The primary technical challenge of the project is to enable the production of small scale cost effective, efficient and reliable units.

The parabolic dish concentrator technology, in particular, has to be improved in terms of concentration ratio increase and weight reduction. With this regard, the partners have considered different design solutions with the aim of increasing the dish performances maintaining a light and handy structure. In particular, since the dish-Stirling manufacturer INNOVA has developed and optimized a small scale system (1 kWe) with a reflecting surface of 10 m² (3.5 m diameter), it has been initially evaluated the possibility of realizing a higher capacity system through the integration of modular units. Therefore different dish configurations have been analysed, with a particular focus on two possible options: multi-dish arrangement, consisting of a structure composed of several dishes, or single dish configuration. Two possible configurations have been considered for the multi-dish arrangement: the “daisy” structure, consisting in a concentrator system composed of several dishes, and the “stand-alone dish array” system, consisting in an array of separate dishes, each connected to a separate receiver. More precisely, in the daisy arrangement four elements are disposed around the tracking axis; each one of the four dishes is suitably oriented to reflect the solar radiation in the same point. In the array configuration each receiver is connected to the others by a pipe line, ending to a common MGT.

With regard to the stand-alone dish array configuration, through a thermal cycle analysis it has been concluded that the presence of the piping network, which connects each receiver to a common MGT, significantly affect the solar to electrical conversion efficiency of the system, increasing, at the same time, the investment costs..

Concerning the daisy arrangement, a ray-tracing based model for the optical characterization of the system has been developed and the results of the optical analysis are reported in the following paragraph. The dish arrangement selected has been subsequently tailored to the MGT-receiver requirements. In particular the solar collector has been optimized in terms of shape for achieving the target concentration factor and turbine inlet temperature.

3.1. Daisy configuration analysis and preliminary design

Very often the size of the solar spot concentrated at the focal plane is calculated by assuming a Gaussian distribution for each parameter. Indeed the Gaussian approach simplifies the treatment by virtue of the property that linear combinations of normal (Gaussian) distributed variables are themselves normal distributed. Two very important parameters are the divergence of the solar radiation and the deviation of mirror shape from an ideal paraboloid. However, in clear sky conditions, the angular distribution of Solar radiation is better approximated by a rectangular rather than a Gaussian function. Moreover, since the surface of the facets composing the reflector is continuous, the shape deviations in two different points of the same facet are highly correlated as they are close to each other; therefore the deviation behaves as a continuous curve with features that are quite systematic for a given production batch of facets. Furthermore, for practical convenience, the mirrored surface of the dishes is very often shaped as an annulus with a missing slice.

With the purpose of evaluating the dish optical features in a rigorous manner, the dedicated software SIMUL-DISH has been developed; it is a cross-platform software (Linux, Mac, Windows), written in C++ with a Qt graphical user interface. The surface of the reflector can be assumed as parabolic or spherical or it can be “customized” by considering the surface (x, y, z and slopes) experimental data as inputs, available once the experimental dish characterization is completed. The flux calculation is performed through a finite element approach. As shown in Fig. 2a the dish surface is divided in annulus, which are projected on the plane xy of the reference frame, where the z axis coincides with the paraboloid axis, and the frame origin is in the vertex. In this frame the projection is exactly circular; the diameter values of inner and outer circles are set according to the chosen numerical resolution (Δs). Then the projected annulus is divided in sectors having radial and angular dimensions close to Δs . It has been found that $\Delta s=10$ mm is sufficient to get accurate results. With the aim of breaking down the computing-time, here a novel hybrid procedure has been adopted: the ray tracing is dealt by considering only the ray travelling along the axis of the cone containing the direct solar radiation (see Fig. 2b); the apex angle is set to the typical divergence of the solar radiation (9.46 mrad); the apex is put in the central point of the considered surface-element; the normal to the element-surface unit vector is obtained by the analytical equation of the surface; the reflection of

the central ray is computed according to the laws of reflection; the intersection point between the reflected central ray and the plane where the virtual charge-coupling-device (CCD), here used for the numerical evaluation of the flux, lies is computed. From this point the procedure becomes analytical with the geometrical computing of the elliptical intersection of the reflected solar beam with the CCD; the counter of all the pixels internal to the ellipsoidal spot is added for the weight $S\cos(\theta_{inc})$, where S is the area of the surface-element, and θ_{inc} the incidence angle of the solar radiation impinging on it.

As shown in Fig. 2b, in the simulation the flux is numerically measured with a 201×201 virtual CCD. The CCD rows (columns) are parallel to the x(y) axis; the CCD surface is parallel to the xy plane, and centred in (0,0,z). Each time the flux ratio entering the circular receiver window (RC) is computed. The flux measurement is repeated for different CCD z-values, spanning a range which is expected to include the optimal z-value. Then the following surface-element is considered, and the computing procedure is repeated.

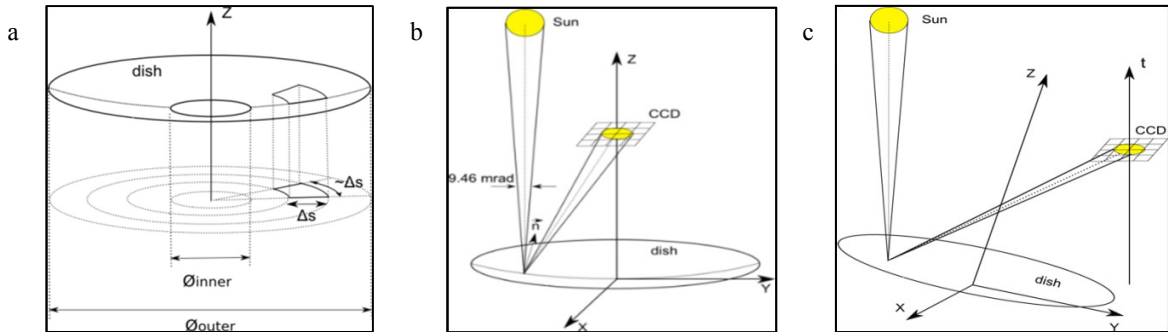


Fig. 2. a) Reflecting surface division in finite elements. b) Flux calculation by a virtual CCD. c) Arrangement of one dish in a daisy configuration.

The optimal position of the receiver is at the z value where RC is maximum. In correspondence of this optimal position the following outputs are given: i) the effective capturing area seen from the Sun; ii) the maximum (C_{max}) and the mean (C_{mean}) values of the concentration factor expressed in Suns; iii) the mean and the standard deviation of the incidence angle of the reflected rays with the receiver window.

SIMUL-DISH can also simulate the “daisy” system, where four replicas of the same dish are arranged around the tracking axis t , with their optical axis directed to the same point t_c . As shown in Fig. 2c, in that case the CCD is placed on the t -axis. To save computing-time, the contribution to the flux of the other three dishes is obtained considering the symmetry of the “daisy”. The first application of SIMUL-DISH was the comparison between the single dish configuration and the daisy-arrangement of four dishes. In both the cases the dish surface is assumed spherical because dishes with quite low ratio aperture/radius-of-curvature are considered. The receiver window diameter is 190 mm. The four dishes composing the daisy are fully mirrored (dark-slice angle 0°) whereas the single dish is mirrored for 11/12 of the circle-angle, equivalent to a dark-slice angle of 30° , in order to ensure the stow position. Another difference is that the single dish is not mirrored in the inner part ($D_{inner} = 1.2$ m), because of the receiver-MGT shadowing. The curvature radius is 14 and 12 m for the single and the daisy-arrangement, respectively: these values are close to those of the 25 kW_e McDonnell Douglas dish and the INNOVA dish, respectively. The outer diameter of the single dish is set to 8 m, to obtain an effective area similar to that given by four INNOVA dishes in the daisy arrangement (see Tab. 1). The results of the optical analysis are synthesized in Tab.1: the RC of the single-dish configuration is higher than the daisy-arrangement and the encumbrance is much less.

Table 1: Optical analysis results: Single Dish vs Daisy arrangement

Simulation	R _{curvature} (m)	D (m)	A _{effective} (m ²)	Z _{receiver} (m)	RC(%)	C _{mean} (Suns)
Spherical_3 (11/12)	14	1.2 - 8.0	45.0	6.75	100.0	1592
Daisy_1 14.00°	12	4.0	48.7	5.25	89.7	1547

In conclusion, from an optical point of view, the single dish option is more efficient than the daisy structure. For its preliminary sizing the following parameters have been assumed: DNI=800 W/m², dish surface utilization factor=80%, maximum electric power output (P_{ele})=10 kW, global solar-electricity conversion efficiency (η_{toi})

=20%. Therefore the resulting dish diameter should be greater than 10 m. In order to keep a margin of flexibility and tolerance in view of possible system modifications, a 12 m nominal diameter dish has been selected, derived from the SunCatcher system developed by Tessera Solar. The main geometrical characteristics of the dish are listed in Table 2.

4. System integration

The demo system has been modelled using both TRNSYS and EES programs with the aim of combining the features of TRNSYS code, which is a quasi-steady simulation model provided with a broad solar thermal electric components library, and the flexibility of the equation solver EES, which can be used for customizing components and control algorithms. In particular TRNSYS code has been initially used for assembling a preliminary simplified tool, using the components available in the TRNSYS library while, in a second step a more customized and detailed system has been built, integrating the components model developed mainly in EES as external subroutines. The present work deals with the refined model, which results from the assembly of different modules, each represented as a box which is described by characteristic equations or performance maps and receives time dependent inputs and produces time dependent outputs. Since the system components are still under development, several assumptions have been made on their design and their performance according to the information currently available.

4.1. Model development

As represented in Fig. 3a, the system model is composed of the following units: dish, receiver compressor, turbine and recuperator. The main parameters assumed for the description of the components performance are reported in Table 2. All the modules are connected within TRNSYS environment, where the DNI measured at ENEA Casaccia site [6] is the time dependent input and the calculation of a self-consistent set of variables at each time step is performed. Each component model, including the control algorithms, has been separately implemented and then integrated into the system. As for the control issue, an algorithm has been conceived for keeping the TIT below the maximum value of 900°C and a second control procedure has been devised for modulating the electrical power output. Regarding the first one, it has been hypothesized to defocus or partially cover the dish when the TIT is higher than 900°C, dumping the exceeding solar power. Concerning the latter one, the MGT speed rate *rpm* has been varied based on the DNI value to maximize the electrical power output, controlling the generator load torque.

Table 2. Model parameters assumed

System Parameters					
Dish external diameter [m]	11.7	Tracking total error [mrad]	7.0	Isoentropic compression efficiency [%]	74.0
Dish internal diameter [m]	2.12	Receiver window radius [m]	0.1	Mechanical efficiency [%]	95.0
Nominal aperture area (m ²)	108.1	Window apparent absorbance	0.9	Isoentropic turbine efficiency [%]	80.0
Effective aperture area (m ²)	96.1	Receiver emissivity	0.9	Electrical efficiency [%]	90.0
Focus quote (m)	7.04	Design mass flow rate [kg/s]	0.1	Recuperator efficiency [%]	85.0
Dish reflection efficiency [%]	92.0	Receiver pressure drop [%]	2.0	Compressor inlet temperature [°C]	15.0
Dish shape factor	0.6	Recuperator pressure drop [%]	2.0		

With regard to the dish component, the ray-tracing model described in the previous paragraphs has not been adopted for the system integration purpose because of its computational burden. A simplified tool, indeed, based on the Gaussian distribution approach has been developed to predict quickly and accurately the optical behavior of the concentration system. The theoretical background of the model is described below.

Since the sun is seen from the earth with a half-opening angle θ_s , the reflected radiation does not affect in a point (the focus) but in a circular area of radius r_g located on the focal plane and said focal spot. In Fig. 3b the geometrical relation between r_g , the diameter D , the focal distance F and θ_s is represented.

Typically the θ_s angle takes into account the natural section of the solar disk (4.7 mrad, 0.27°) increased by the contribution of the error on the shape of the mirrors, the imperfect specularity of the mirrors, the diffractions, the pointing errors and those concerning the alignment in the positioning of the mirrors and the receiver. Such errors are seen statistically independent so that the actual value of θ_s is the square root of the sum of the squares of the individual errors. This value θ_s can be considered equal to about 7-10 mrad (0.4°-0.57°) [7] and it can take into

account also the fluctuations due to the imperfections of the reflecting surface.

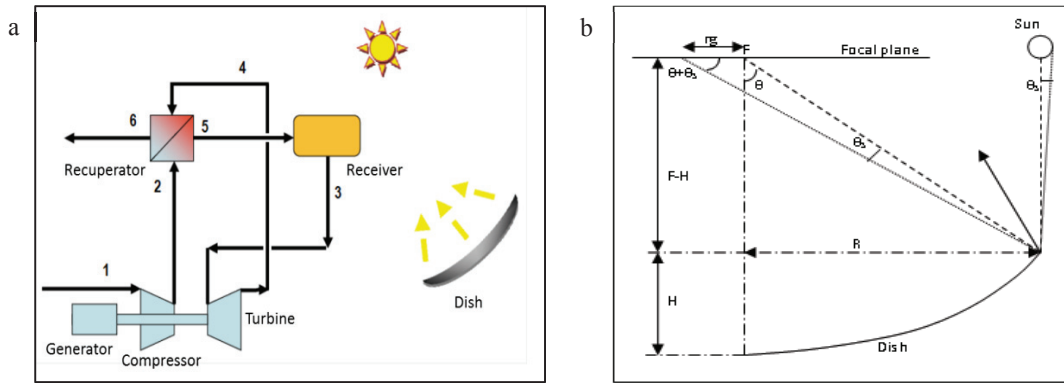


Fig. 3. (a) Scheme of the components integration; (b) Scheme of concentrator reflection

Actually the concentrated solar flux $\phi(\xi)$ on the focal plane, where ξ is the diameter of the focal spot, is not homogeneous and can be described by a Gaussian distribution characterized by the standard deviation μ and the peak flux ϕ^{peak} . If ξ is infinite, P_{in} is the total incident power on the focal plane, whereas, having the window a finite radius r , the incident power on the receiver window P_w can be calculated through the following relation

$$P_w = P(\xi = r) = 2\pi\mu^2 \phi^{peak} \left(1 - e^{-\frac{r^2}{2\mu^2}} \right) \tag{1}$$

On the base of a numerical comparison between the simplified model and a ray tracing optical model, an empirical correlation between the standard deviation μ e r_g , ($r_g=3\mu/2$) has been identified [8]. Therefore it is possible to evaluate the parameters characterizing the flux distribution on the focal plane as a function of the dish geometry, the total tracking error, and the receiver window radius, with the peak flux ϕ^{peak} expressed by the following relation

$$\phi^{peak} = \frac{P_{in}}{2\pi\mu^2} = \frac{\eta_r P_{coll}}{2\pi\mu^2} = \frac{9}{32} \frac{\eta_c DNI}{(r_g / D)^2} \tag{2}$$

where η_r is the efficiency of the reflective surfaces (reflectance) and P_{coll} the power collected on the mirror surfaces.

As shown, the peak flux is a function only of the shape factor $f(r_g/D)$ and the half angle θ_s and independent of the diameter of the concentrator. This last, however, affects the width of the distribution and then the radius of the receiver window. On the basis of the equation (1) and (2) it is possible to evaluate, accurately enough, the optical performance of a PDC (incident power on the receiver window P_w) as a function of the dish geometry, total tracking error, and the receiver window radius.

Regarding the receiver module, a cavity receiver with an aperture window radius r has been assumed for the modelling purpose and the following heat balance equations have been considered for the calculation of the power absorbed by the air flow P_{net} (see Fig. 3a for the process scheme) :

$$P_{net} = P_{abs} - P_{reirr} - P_{conv} = m_{air} \cdot (h_3 - h_5) \tag{3}$$

$$P_{abs} = \alpha \cdot P_w \tag{4}$$

$$P_{reirr} = \varepsilon \cdot \sigma \cdot A_w \cdot (T_3^4 - T_{sky}^4) \tag{5}$$

$$P_{conv} = U_{conv} \cdot A_w \cdot (T_3 - T_a) \tag{6}$$

where P_{abs} is the power transmitted to the cavity, α is the global apparent absorbance of the window, P_w is the incident power at the receiver window, P_{reirr} is the power lost by radiation, ε is the receiver emissivity, σ is the Stefan-Boltzman constant, T_3 is the receiver temperature assumed constant and equal to the outlet air temperature, T_{sky} is the reference temperature for radiation phenomenon (15°C), T_a is the ambient temperature, P_{conv} is the power lost by convection from the window surface, A_w is the window aperture area, m_{air} is the air flowrate, h_5 and h_3 are the inlet and outlet air flow enthalpies, respectively, and U_{conv} is the heat transfer coefficient for natural convection from the aperture window, neglecting the convective losses from the insulated cavity sections, and has been calculated from the correlation [9]

$$U_{conv} = b \cdot (\Delta T_f)^m L^{3m-1} \tag{7}$$

where b (1.32-1.37) and m (0.25) are empirical parameters which depend on the fluid properties and system geometry, ΔT_f is the temperature difference between hot surface and ambient temperature, L is the system characteristic dimension. The model, which in a first approximation doesn't take into account the receiver thermal inertia, has been written in EES and integrated into the system model as an external subroutine.

Regarding the micro gas turbine system, as already mentioned, it is composed of a compressor, a turbine, a recuperator and a generator. The turbine shaft work is used to drive the compressor and the electric generator that is coupled to the shaft. Since the MGT component is currently under development and no detailed information are available, the performance map approach has been selected for modeling the compressor and the turbine operation. In particular the performance maps represented in Fig. 4a and Fig. 4b, derived from an existing design proposed by Compower, have been considered for the calculation of the turbo-compressor operating point. In Fig. 4a the compressor pressure ratio P_{ratio} (P_2/P_1) is plotted against the compressor corrected mass flow m_{air-c} at different speed rate rpm while in Fig. 4b the turbine expansion ratio P_r (P_4/P_3) is plotted against the turbine corrected mass flow m_{air-t} . The turbo-compressor operating point has been individuated by matching the air flow rate m_{air} and the pressure ratios P_{ratio} and P_r , net of the cycle pressure drops.

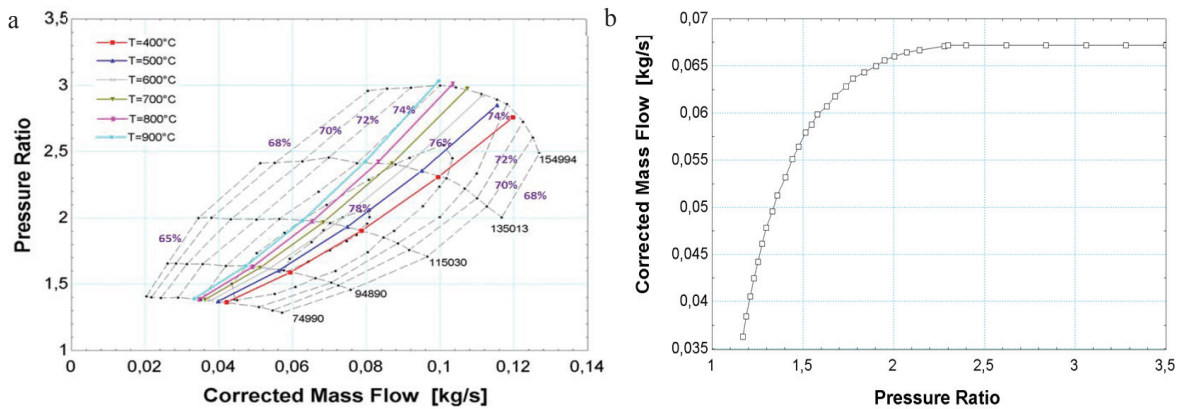


Fig. 4. (a) Compressor performance map [10]; (b) Turbine performance map [10]

Furthermore, since the driving torque and the load torque are perfectly balanced in the steady state condition, the electrical power output P_{ele} is equal to the turbo-compressor net power, as reported in the following relation

$$P_{ele} = (P_t - P_{cm}) \cdot \eta_{ele} \tag{8}$$

where η_{ele} is the electrical efficiency and P_t and P_{cm} are the total turbine and the total compressor power, respectively. Concerning the recuperator, it has been assumed, as a preliminary approximation, that the heat exchange efficiency η_{rec} has a stepwise behavior, being 0.85 for a turbine outlet temperature equal or higher than 160°C and 0 in correspondence of a temperature lower than 160°C.

In conclusion, for the MGT model implementation, the following equations have been considered (Fig. 3a):

Table 3. MGT heat balance equations

Compressor	Recuperator	Turbine
$P_{cm} = \frac{P_c}{\eta_{mec}} = \frac{m_{air} \cdot (h_2 - h_1)}{\eta_{mec}}$ (9)	$P_{rec} = m_{air} \cdot (h_5 - h_2)$ (11)	$P_t = m_{air} \cdot (h_3 - h_4)$ (13)
$\eta_c = \frac{(h_2 - h_1)}{(h_{2is} - h_1)}$ (10)	$\eta_{rec} = \frac{T_5 - T_2}{T_4 - T_2}$ (12)	$\eta_t = \frac{(h_3 - h_4)}{(h_3 - h_{4is})}$ (14)

where, P_c is the power absorbed by the compressor, net of the mechanical efficiency η_{mec} , h is the air flow enthalpy, h_{is} is the isentropic air flow enthalpy, η_c and η_t are the compressor and the turbine isentropic efficiencies, respectively, and P_{rec} is the recuperator power.

4.2. Simulation results

The implemented model has been initially applied to perform a parametric analysis to evaluate the system performance at different DNI values and different generator speed rates. The simulation results are reported both in Fig. 4a and Fig. 5a. In particular in Fig. 4a a set of isothermperature working lines, corresponding to different TIT, has been included in the compressor performance map: at each temperature level a different MGT working point can be identified varying the MGT speed rate. Clearly every working point is characterized by a specific electrical power output, as represented in Fig. 5a, where the electricity production is correlated to the DNI and the MGT speed rate. From the Fig. 5a it is evident that the power output is constantly positive for DNI values higher than 400 W/m². Furthermore it clearly emerges that, at a fixed MGT speed rate, the power output raises as the DNI increases up to the maximum value in correspondence of a TIT of 900°C: for higher DNI values the control system keeps the TIT constant by a defocus procedure or a mirror partial covering method. An envelope has been created considering the parametric curves of Fig. 5a with the aim of maximizing the power output at each DNI level. The resulting curve, represented in Fig. 5b, allows to correlate the MGT speed rate n with the DNI and, consequently, to define a control strategy to optimize the MGT operation. The resulting power output P_{ele} is represented in the same Figure.

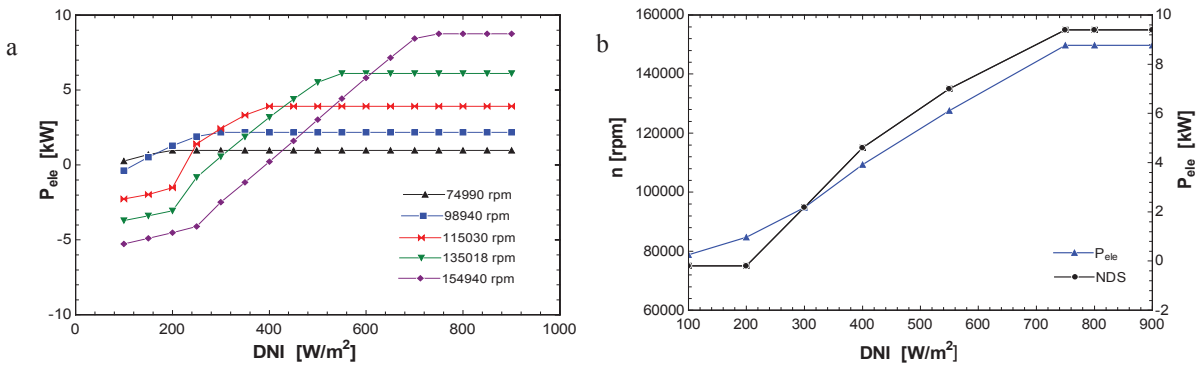


Fig. 5. (a) Electrical power output as a function of DNI and system speed rate ; (b) Optimal working lines

On the basis of the rpm-DNI correlation above mentioned, the model has been applied to describe the system daily operation, even in off-design conditions, i.e. with the TIT and the mass-flow rate below 900°C and 0.1 kg/s, respectively. The DNI course measured in July 2011 at ENEA Casaccia site [6] has been considered as an example to simulate the operation of the plant from the start-up to the shut-down..

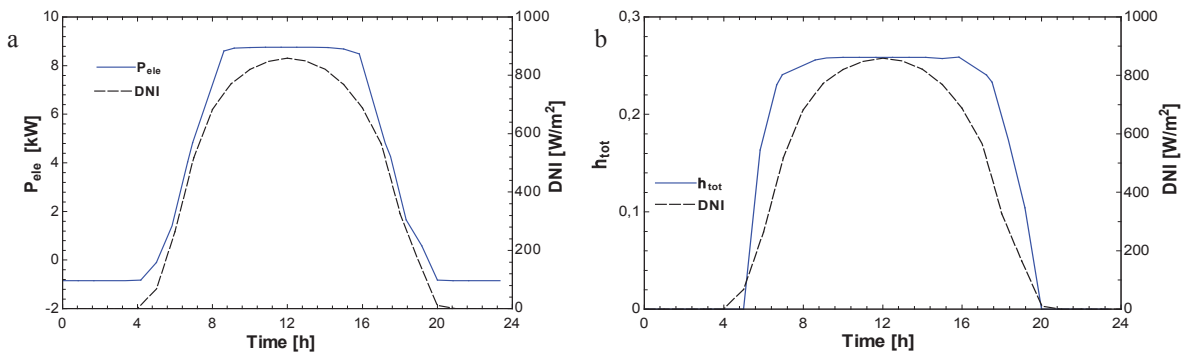


Fig. 6. (a) Power output vs time; (b) System total efficiency vs time

The system performance in terms of electrical power produced vs time and system total efficiency vs time is represented in Fig. 6a and Fig. 6b, respectively, while the TIT course and the compressor pressure ratio course are represented in Fig. 7a and 7b. The daily solar to electricity conversion efficiency in this case is about 10% but the analysis will be extended to an yearly basis in order to get more extensive and meaningful data for the

implementation of the control strategy and for improving the components design. Once the components are developed and tested, it will be possible to further refine the system model through the adoption of updated data and experimentally validated performance curves. The possibility of integrating a thermal storage into the demo system will also be investigated converting the quasi steady state approach into a more realistic dynamic analysis

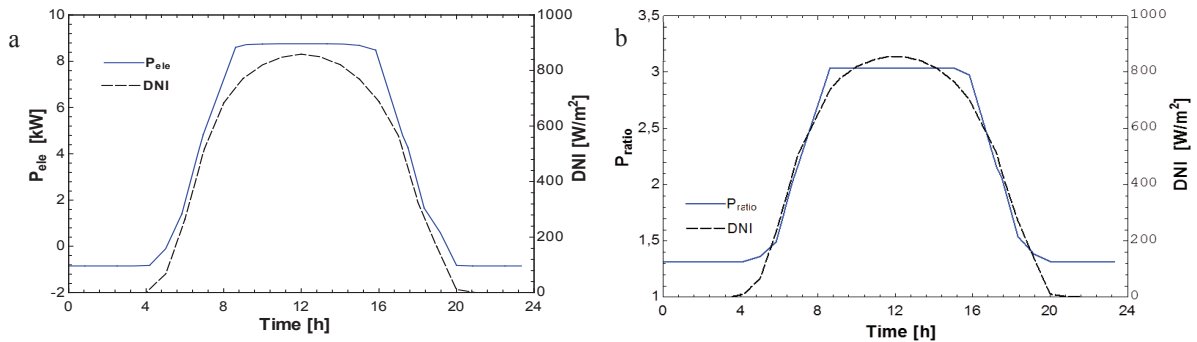


Fig. 7. (a) Turbine Inlet Temperature vs time; (b) Compressor pressure ratio vs time

5. Conclusions

In the frame of the European funded OMSoP project, a demonstrative plant which integrates the solar dish technology and a MGT system for renewable electricity production is being developed. The partners are currently involved both in the components development and in the system analysis activity. With regard to the components development, ENEA has contributed to the preliminary design of the solar dish through a theoretical analysis aimed at evaluating the best dish configuration in terms of optical efficiency. With this purpose different optical models have been implemented and the analysis has been focused on two possible options: multi-dish arrangement, consisting of a structure composed of several dishes, or single dish configuration. The single dish arrangement, which has been selected as the most efficient and reliable, has been subsequently tailored to the MGT-receiver requirements. Furthermore the dish optical models have been applied for the realization of a complete system model for the simulation of the demo plant. The obtained results show that the implemented model can be used for the analysis of the daily system operation even in off design conditions. As a further step the system analysis will be extended to a yearly basis both for predicting the behaviour of the demo plant and for guiding the system components improvement.

Acknowledgements

The authors wish to acknowledge the financial support from the European Commission within the 7th Framework Programme, through project OMSoP - Optimised Microturbine Solar Power system (Contract No 308952).

References

- [1] SOLGATE project: "Solar hybrid gas turbine electric power system project report", http://ec.europa.eu/research/energy/pdf/solgate_en.pdf
- [2] SOLHYCO project: <http://www.greth.fr/solhyco/>;
- [3] SHCC project: http://www.vgb.org/en/research_project327-path-1,2128.html;
- [4] Quero, M, Korzynietz R, Ebert M, Jiménez AA, Del Río A, Brioso JA, Energy Procedia, "Solugas - Operation experience of the first solar hybrid gas turbine system at MW scale", 49, 2013, p. 1820-1830;
- [5] PEGASE project: <http://www.fp7-pegase.com/>
- [6] Spinelli F, Cogliani E, Maccari A, Milone M, La misura e la stima della radiazione solare: l'archivio dell'ENEA e il sito Internet dell'Atlante italiano della radiazione solare per la pubblicazione dei dati, Energia Ambiente e Innovazione, ENEA, 1/2008;
- [7] Stine WB, and Harrigan R, Solar Energy Fundamentals and Design with Computer Applications. New York: Wiley-Interscience, 1985;
- [8] Crescenzi T, Lanchi M, Miliozzi et al., OMSOP Project, Report D1.5 "Optimized dish design", January 2014;
- [9] Perry RH, Green D, Perry's Chemical Engineers' Handbbok, McGraw-Hill Book Company, 1994, p. 10-13;
- [10] Malmrup L., 2013, private communication.